Suppression of Harmonics in Microstrip Filters Using a Combination of Techniques

Huang, Frederick

DOI:
10.1109/TMTT.2015.2461616

Document Version
Peer reviewed version

Citation for published version (Harvard):
Huang, F 2015, 'Suppression of Harmonics in Microstrip Filters Using a Combination of Techniques', *IEEE Transactions on Microwave Theory and Techniques*, vol. 63, no. 10, pp. 3453-3461.
https://doi.org/10.1109/TMTT.2015.2461616

 IEEE Trans. on Microwave Theory and Techniques, 2015 or 16.
DOI 10.1109/TMTT.2015.2461616. Will be available on IEEE Xplore.

Suppression of Harmonics in Microstrip Filters Using a Combination of Techniques

Frederick Huang

***Abstract*— Existing and newly-adapted techniques for suppressing harmonic responses in microstrip filters were combined. Stagger tuning using additional stubs to shift the resonances has been adapted to quarter-wave resonators and extended to the 7th order spurious response. Suitable resonator overlap provided transmission zeroes to cancel spurious peaks. Coupling capacitor pads acting as shorting stubs have been developed. Spurious responses were suppressed to better than -33 dB, up to 6.3 GHz, in a measured filter with 1 GHz center frequency and 42% bandwidth. Suitably placed resistors have depressed the spurious level further to -50 dB up to 5.6 GHz, with only 0.07 dB extra pass band loss.**

***Index Terms*—harmonic suppression, microstrip filters, resistive attenuation, resonator overlap, spurious response suppression, stubs.**

I. Introduction

THE stop band of distributed filters, including microstrip band pass filters, is often limited by harmonic or other spurious responses. There are a large variety of methods of suppressing them, as listed in many papers including [1]. The aim of the present work is to combine some of these techniques to achieve a high level of suppression over a wide bandwidth. Quarter-wave resonators are employed, so some adaptation is required. Even order resonances are not present, so the aim was to suppress the third, fifth and seventh order responses. Wide bandwidth filters, such as the ones described here, often have strong coupling at the harmonics as well as the pass band, so it is a greater challenge to suppress them.

The first technique uses resonators with the same fundamental but different higher order resonances, that is, stagger tuned spurious peaks. Previously, this was done with stepped impedance resonators with differing characteristic impedances or differing lengths of high- and low-impedance sections [2]-[4]. Even without stagger tuning, the stop band may be widened, because the spurious responses are shifted [5], [6]. Additional stubs can also shift the resonances [7], [8]. Stubs or other resonators may introduce transmission zeroes [9], [10], but further resonances may be introduced, which have to be stagger tuned. In [1], stubs, approximately quarter wavelength at the third harmonic, caused the 2nd and 3rd resonances to differ between resonators. The type of main resonators can be chosen independently from the stubs, for compactness, or low loss, or insensitivity to over-etch. The design equations will be adapted for quarter-wavelength resonators, and examples for use in filters provided.

The second technique, adopted with little change, is to adjust the overlap between two parallel-coupled resonators for minimal coupling at the spurious frequencies [11], [12], [13], [14], and [15]. In [11] two suppression techniques are also used simultaneously. A variant is [16], where the section of input line that overlaps the first resonator is not at the end of the line, but set back by a predetermined distance.

One way of coupling two quarter-wavelength resonators is to join one end of each resonator to a capacitive pad instead of earth; a larger capacitance implies smaller coupling. This suppresses the higher order responses, since the capacitance acts more like a short circuit as frequency is increased. With a poor design, for example if the capacitance forms a half-wave resonator, this effect can be lost, but on the other hand it can be enhanced if the pad acts as a quarter-wave resonator to short-circuit a spurious response [7]. The resulting transmission zeros can also be used to tighten the pass band skirts [17], [18] or make a general improvement in the stop band attenuation [19]. The resonating pads used in this paper are very wide, as required for a suitable pass band coupling coefficient, introducing an additional issue which will be discussed.

Two quarter-wave resonators together with their connecting pad form a dual mode resonator utilizing symmetric and anti-symmetric modes. In this sense, the filter is a small first step towards using stubs to attenuate spurious responses in multimode resonators such as in [20].

Resistive attenuation that is significant only in specific resonator modes [21]-[23] was adopted in one of the filters.

Two further techniques are not closely related to the present work but their results will be compared. Wide pass-band filters can be implemented using stubs and 90 degree transmission line phase shifters. Spurious responses can be suppressed with stepped impedance phase shifters or transmission lines with more stubs [24] – [26]. The other technique uses stepped impedance resonators with a very low impedance ratio, and interdigital capacitive coupling [27].

Submitted 23 Jun 2014.
F. Huang is with the University of Birmingham, UK, (phone: UK (0)121-4144299; fax: UK (0)121-4144291; e-mail: f.huang@bham.ac.uk).

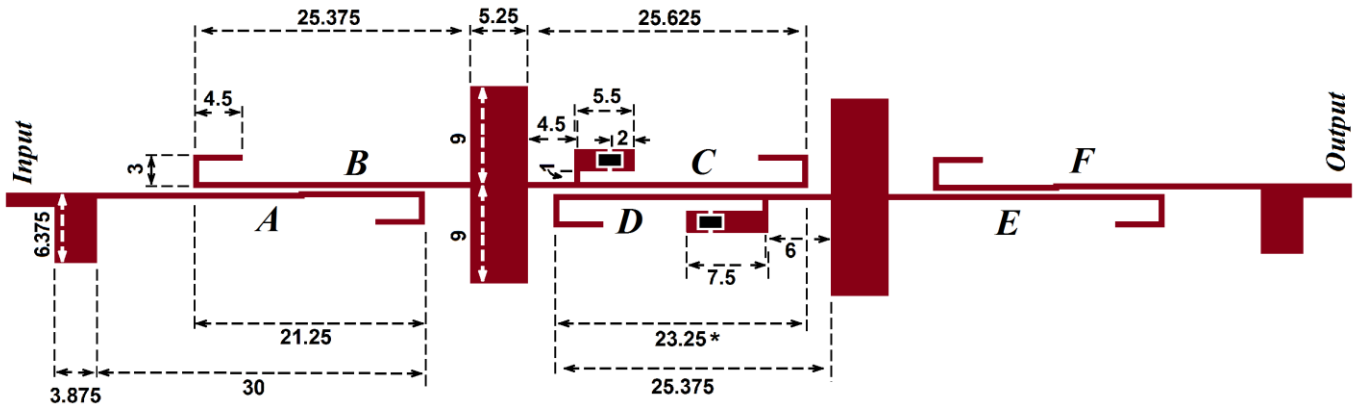

Fig. 1. Filter layout. Dimensions in mm. In the first filter, the dimensions are as shown except the overlap 23.25* is 23 mm, and the stubs on resonators C and D are continuous copper strips. In the second, all the dimensions are as shown and the stubs include breaks, which are bridged by 20 Ω resistors shown as black rectangles.

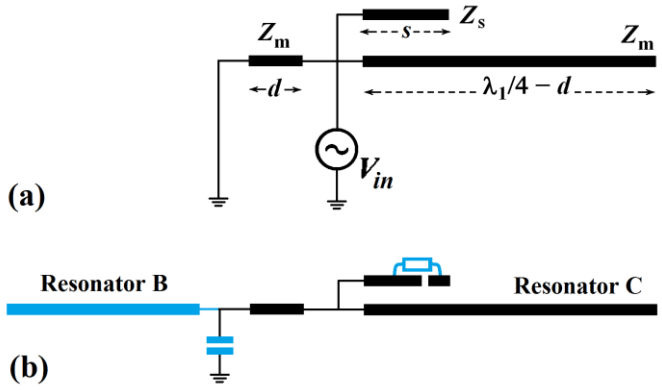

Fig. 2(a). Transmission line model of a quarter-wave resonator with a stub, analyzed as a 1-port circuit. (b) Incorporation of the quarter wave resonator into a pair of coupled resonators. The resistor is added only in filter 2; neither resistor terminal is earthed.

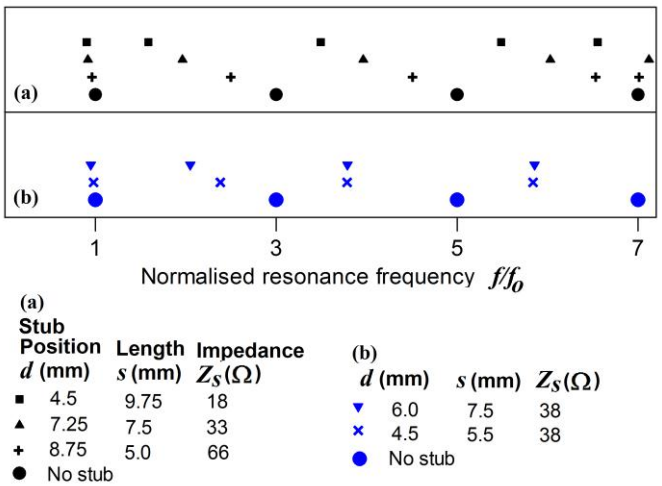

Fig. 3. Computed resonances of quarter-wavelength resonators with stubs. For clarity, the resonances of each resonator are separated vertically; there is no other significance of the vertical scale. The main line has characteristic impedance $Z_m = 72$ Ω. (a) A possible set of stubs giving all-round stagger tuning. (b) Stubs used in this work, where additional suppression is also used.

Two similar sixth order, quarter-wave microstrip 42% bandwidth filters centered at 1 GHz were designed, fabricated and measured. The second is illustrated in Fig. 1, with the small differences between them noted. Resonator A is coupled to the input via a capacitive pad, while B and C are similarly joined. Resonators A and B are parallel coupled, as are C and D. Resonators E and F are identical to B and A when the filter is rotated through 180 degrees, and the capacitor between F and the output is a mirror image of A and the input. Thus the filter is electrically symmetrical except for center resonators C and D, which have different lengths and differing stubs.

The design process relies heavily on iterative simulations, but some approximate design equations greatly assist by providing a close starting point, and qualitative insight helps in the iterative process. Analytic equations to optimize the filter as a whole, or to provide a precise trade-off between various requirements, or to choose a complementary set of suppression techniques, are too ambitious for the present. Estimating the achievable level of suppression has proved difficult in the past [1] because of low-level coupling between non-adjacent resonators, and was not attempted here.

II. Stagger Tuning Using Stubs

The transmission line model of a resonator with a stub is shown in Fig. 2(a). The main line has characteristic impedance Z_m, and unlike [1], has one end shorted. An additional stub of length s and tap position d has characteristic impedance Z_s. The normalized input susceptance seen by the source is

$$\frac{Y_{in}}{jY_m} = \tan\left[2\pi f\left(\frac{\lambda_1/4-d}{v}\right)\right] + \cot\left[2\pi f\frac{d}{v}\right] + \frac{Z_m}{Z_s}\tan\left[2\pi f\frac{s}{v}\right] \quad (1)$$

where v is the propagation velocity and λ_1 is the wavelength of the fundamental frequency. As in [28] and [1], resonance occurs when this is zero. By selecting appropriate values of d, s and Z_s in trial and error calculations, the frequencies of the 3rd, 5th and 7th order resonances are chosen, with minimal

effect on the first order resonance. In Fig. 3(a), the well separated resonances of a set of four stagger tuned resonators are shown, very useful if this technique were used by itself.

However, the present work also exploits transmission zeroes arising from the other suppression techniques, so the resonances can cluster around them and still be attenuated. This allows a filter design that is only slightly asymmetrical. Relinquishing one degree of freedom, by using equally wide stubs, allows more space to mount resistors. The choice is shown in Fig. 3(b). The resonances of resonators C and D (triangles and crosses) are separated from the four others (all approximated by the circles) which cluster around transmission zeroes. It was not found necessary to separate the higher order resonances of C and D. Resonators are coupled when they share a capacitive pad, as shown in Fig. 2. This may cause the resonances to shift, necessitating iterative simulations in the filter design.

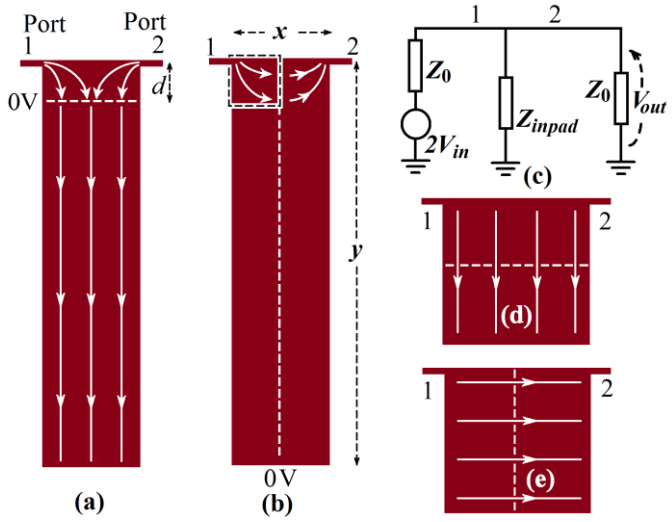

Fig. 4. Coupling capacitance pads. (a) Current distribution for symmetric excitation in a narrow pad. (b) Antisymmetric excitation. (c) External circuit for single-sided excitation. (d) and (e) Current distribution for a square, half-wavelength pad.

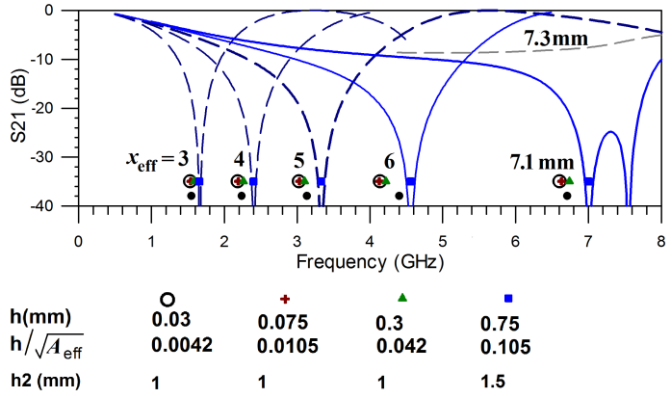

Fig. 5. Simulated center frequencies of notches due to resonating capacitive pads, as shown in Fig. 4. Z_0=50 Ω. Effective resonator length is y_{eff}=50/x_{eff} mm. Dark and mid-blue lines: Response S_{21} for h = 0.75 mm. Black dots: Estimate from eq. (4).

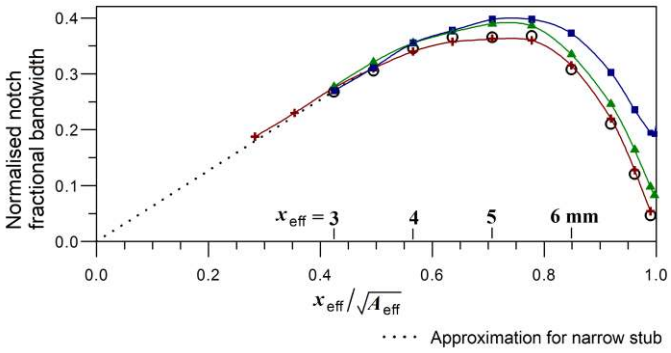

Fig. 6. Simulated values of normalized notch fractional band width for various dielectric thicknesses and capacitance pad widths. Effective area $A_{eff}=y_{eff}x_{eff}$ of the pad is 50 mm^2. The legend is given in Fig. 5.

III. Resonator Overlap

For the present paper, the appropriate overlaps for zero coupling between resonators A and B, and between C and D, at a particular frequency were found from electromagnetic simulations. As in [12], the lines were shortened with hairpin bends near their open ends, in this case at an arbitrary position, but consistent with leaving space for the stubs. For second harmonic suppression [11], [13], [14], [15], the required overlap exceeds a quarter fundamental wavelength, but the overlap is less for the third harmonic so there is no unwanted contact between resonators and nearby capacitor pads. Good suppression depends on accurately fabricating the overlap, which becomes difficult at higher frequencies, so this technique is usually best for the lowest order spurious resonance.

IV. Resonating Coupling Capacitor Pads

The coupling pads placed for example between input and resonator A, or between B and C, behave at higher frequencies more like stubs than pure capacitances (not to be confused with the stubs in section II). A narrow resonating pad is shown in Fig. 4(a-c). When y approximates a quarter wavelength, the magnitude of the pad input impedance is $|Z_{inpad}| \approx \left|Z_{0pad}\cot\left(2\pi f\frac{y_{eff}}{v}\right)\right| \ll Z_0$, where y_{eff} is effective length of the pad, including an allowance for fringing fields and Z_{0pad} is the characteristic impedance of the pad behaving like a wide transmission line. The left-hand and center impedances in fig. 4(c) form a potential divider, which is not significantly loaded by the right-hand impedance, so

$$\left|\frac{V_{out}}{V_{in}}\right| \approx \left|\frac{2Z_{0pad}}{Z_0}\cot\left(2\pi f\frac{y_{eff}}{v}\right)\right| \quad (2)$$

The cotangent gives a constant notch fractional bandwidth as y_{eff} is decreased and the quarter-wavelength resonance frequency is increased. However, for a given pass band coupling coefficient, the area A of the pad (or strictly speaking the effective area, allowing for charge concentration at the edges) should be approximately constant. Therefore x is increased and Z_{0pad} is decreased. The notch fractional bandwidth then increases and suppression improves as the resonance frequency is increased, up to a limit to be described, and this technique is a complement to the resonator overlap since it is usually more effective at high frequencies.

The criterion for effective suppression is not zero or infinite input impedance, but a near-zero output, when the magnitudes of the input voltages for symmetric and anti-symmetric excitation shown in Fig. 4(a) and (b) are equal. The dashed square on the top-left-hand side of (b) has zero voltage on the right-hand side, zero current crossing on the left-hand edge and the top edge, and only a small current crossing the bottom. When rotated clockwise by 90 degrees, it is similar to the pattern on the top right hand side of (a). A further reason why this is only approximate is that the line of zero voltage in (a) is not perfectly straight. This observation gives the crude approximation

$$d \approx x_{eff}/2 \tag{3}$$

So the condition for zero output is

$$\frac{\lambda}{4} \approx y_{eff} - \frac{x_{eff}}{2} \tag{4}$$

where x_{eff} and y_{eff} are the effective values of x and y, allowing for the fringing fields. This is not suggested as an accurate design equation, but as a starting point for simulations, and to enable pass band characteristics to be adjusted iteratively without significant change in the stop band nulls.

For the range $0<x_{eff}<y_{eff}$, the useful frequency range is doubled because of the $x_{eff}/2$ term. Ignoring $x_{eff}/2$ leads to an error up to a factor of 2.

The circuit in Fig. 4(a-c) was simulated and the responses given in fig. 5. Higher order resonances have been deleted for clarity. The idealized substrate of thickness h mm has dielectric constant 10.2 but zero loss, and the metal is also lossless. On top of the metal, a dielectric overlay h_2 with the same dielectric constant avoids a variable effective permittivity, because the electric field lines from the top of the pad to earth are confined to just above the pad and near the edges. Having the whole box filled with the same dielectric is not acceptable because the box resonance frequencies are brought down to the range of interest. The data are not directly applicable to the final filter, but the filter pads are easily studied in further simulations. Based on the values of characteristic impedance given by the electromagnetic simulator SONNET of a transmission line with width x or y,

$$x_{eff} \approx x + 2h \tag{5}$$

$$y_{eff} \approx y + 2h \tag{6}$$

where h is the substrate thickness. They are valid for relatively small values of x and y close to $1.2h$, where the $2h$ correction is needed most. $2h$ is somewhat large because of the greater charge on the top face of the pad, caused by the overlay.

Simulated responses are given in Fig. 5, for h=0.75 mm. Only the simulated notch frequencies are given for the other values of h. They have very good agreement with (4), which is also shown. This is because when the second term in (4) is small, so is any associated error. On the other extreme, with x_{eff} and y_{eff} both half a wavelength, the current patterns are the expected half-wavelength patterns shown in figs. 4(d) and (e), and (4) is again accurate, even though the foregoing arguments incorrectly suggest that Fig. 4(e) is should be similar to 4(b), with current absent in the lower half.

The spread of resonances in Fig. 5 for $x_{eff} = 7.1$ mm is almost identical to those in simulations of patch resonators with capacitive gaps at the input and output, showing that this spread is not due to an error in (4). It is probably because of the simplified value of effective dimensions in (5) and (6), or because the corners also have fringing fields, not accounted for. Thus the error in (4) is small, of similar magnitude to errors in the effective dimensions.

Fig. 6 shows the normalized notch fractional bandwidth $\frac{1}{S_{21}}\frac{Z_{02pad}}{Z_0}\frac{B}{f_0}$, for varying x_{eff}. B is the width of the notch centered at f_0, measured at level S_{21}, (in linear units, not dB, and $S_{21}\rightarrow 0$). Z_0=50 Ω is the impedance of the input and output, and $Z_{02\text{pad}}$ is the characteristic impedance of the resonating pad when $x_{\text{eff}} = \sqrt{A_{\text{eff}}}$. It shows that notch fractional bandwidth is best when $x_{eff} \approx 0.7\sqrt{A_{eff}} \approx 5$ mm. A possible exception is shown in Fig. 5. When h = 0.75 mm, and x_{eff} increases to 7.1 mm, two resonances approach each other and form a wider dip. However, at x_{eff} = 7.15 mm, the two dips combine into one, and when x_{eff} = 7.3 mm, it is very shallow. This implies sensitivity to fabrication error, so it is not pursued for the moment. The exact transition point depends on h. Furthermore, for large values of x_{eff}, the harmonics are not well suppressed.

Varying h effectively varies the ratio between Z_0 (kept at 50 Ω by adjusting the input line width) and $Z_{0\text{pad}}$. Together with the variable $x_{eff}/\sqrt{A_{eff}}$, the main parameters have been considered. At lower values of h, 0.03 and 0.075 mm, the data almost coincide, strongly suggesting that a limiting value has been reached. At the other end of the range, the next value after h=0.75 mm would be 3 mm, which is approaching a quarter wavelength. The extra border added to allow for the fringing field would also be close to a quarter wavelength, so no reasonable results can be expected. Furthermore, for the right-hand side of Fig. 6, x and y would have the similar values to the width of the input line, that is, the pad would not exist. On the left-hand side, (4) is adequate without the second term.

Factors that have a minor influence on the notch frequency and width are the positions of the input and output taps (which currently are not perfectly centered at the corners as they do not join at a 45 degree angle), the thickness of the overlay, and the simulation box dimensions.

V. Resistors in Stubs

With tap positions and stub widths already determined, they cannot be varied to optimize resistive attenuation as in [23]. In compensation, stagger tuning results in narrow spurious peaks that are more easily dealt with by the resistances.

In contrast to [22] and [23], the resistive elements are placed close to the open ends of the stubs instead of near the taps. Assuming that the current distribution is not significantly affected by the resistor, the current in the stub at a distance z from the open end has the form of a standing wave,

$$I(z,t) = I_0 \sin\left(2\pi f \frac{z}{v}\right)\sin(2\pi f t) \tag{7}$$

where I_0 is a constant. Moving a resistor to larger z, current increases almost linearly for the fundamental resonance, but for the higher order resonances, the current magnitude levels off, so the attenuation at the fundamental frequency increases faster than that at the spurious frequencies. A smaller z is therefore a better choice. The improvement may be substantial

elsewhere, but modest here since the worst spurious frequency is only twice the pass band center, and the stubs are relatively short. Additional practical advantages are a more convenient position for the resistor with less perturbation of the main line with the unpredictable solder joint, and lower inductance effects due to the resistor and solder joints. The assumption that *R* does not affect the current is not valid when it is placed at a quarter-wavelength away from the open end, since it dominates the line input impedance. Thus the earlier choice of resistors [22], [23] at the tap is not being reassessed here.

With the current-squared dependence of power dissipation, the same stub characteristic can be obtained by replacing *R* with another series resistor $R \sin^2\left(2\pi\frac{fz}{v}\right) / \sin^2\left(2\pi\frac{fs}{v}\right)$ at the tap, whose value is different for each resonance, and is smaller for the fundamental frequency as described above. The normalized input susceptance of the stub is then

$$\frac{Y_{stub}}{jY_m} = \frac{Z_m}{Z_s \cot\left(2\pi\frac{fs}{v}\right) + jR \sin^2\left(2\pi\frac{fz}{v}\right) / \sin^2\left(2\pi\frac{fs}{v}\right)} \qquad (8)$$

Replacing the last term in (1) with this expression, new Q factors of each resonance of a filter could be estimated. Meanwhile the simulated response of an existing filter gives the existing Q-factors and attenuation levels. From the new Q factors, the new attenuation level can be estimated [22], [23], but the stub lengths and positions do not permit the same simplifying approximations and it is probably more convenient just to re-simulate the filter.

The following rule of thumb is probably more useful in iterative design. Based on [29], the additional pass band loss due to reduced resonator Q factor (not loaded by input, output or other resonantors) varies as

$$L \sim \frac{1}{Q_u} \qquad (9)$$

Pass band attenuation varies approximately linearly with $1/Q_u$ i.e. with *R*, even when measured in decibels [29], because the log scale is nearly linear for small attenuations, as in the pass band where the main resistances are the source and load. In the stop band, if the existing losses are small compared with the resistor loading, a further doubling of the resistance will halve the current and the output at resonance, so output falls by 6 dB. Thus resistance has to rise exponentially for successive equal decrements (in dB) of spurious peaks.

VI. Filter Simulations

Two similar 6th order filters with 1 GHz center frequency and 42% bandwidth were designed. The first filter uses stagger tuning, resonator overlap and resonating capacitor pads, but not the resistive attenuation. The design procedure begins with the pass band, the required coupling coefficients having been found from [30]. The relation between achievable coupling coefficients and dimensions were found from simulations described in the appendix. Filter dimensions were adjusted by repeated iterative simulations. Other passband design procedures could have been substituted. CPU time is a few minutes per iteration.

Turning to the stop band, the overlap between A and B, and between E and F, produce transmission zeroes close to 2.6 GHz, to attenuate their resonances. C and D with their stubs resonate close to 2 GHz, and the overlap was adjusted to attenuate these peaks. There is little change in the pass band provided that the overlaps were already approximately correct, as described in the appendix. To minimize the fifth order response, the dimensions of the two central pads were adjusted, keeping the area of the pads constant to reduce the change in the pass band. This requires a minor iterative loop because the exact positions of the peaks vary with the pad dimensions. Similarly, the two outer pads were adjusted to minimize the 7th order response. Adjustments of the 5th and 7th order responses do not significantly affect the 3rd order adjustments, nor each other. CPU time was a few hours per simulation because of the wider frequency range and the higher frequencies, but only a few iterations were required.

Returning to the pass band for a second set of iterations, adjusting the gaps has very little effect on the stop band; similarly the pad dimensions *x* and *y* were varied in accordance with (4) to keep the notches at the 5th or 7th spurious frequency constant, again so that suppression is approximately unchanged.

Typically, a final fine-tuning of the stop band was sufficient to produce the results to be presented. The procedure is summarized in Fig. 7, showing its simplicity. The number of times round the loop is small because the pass band and stop band iterations do not interfere with each other significantly; (4) plays an important part as described above.

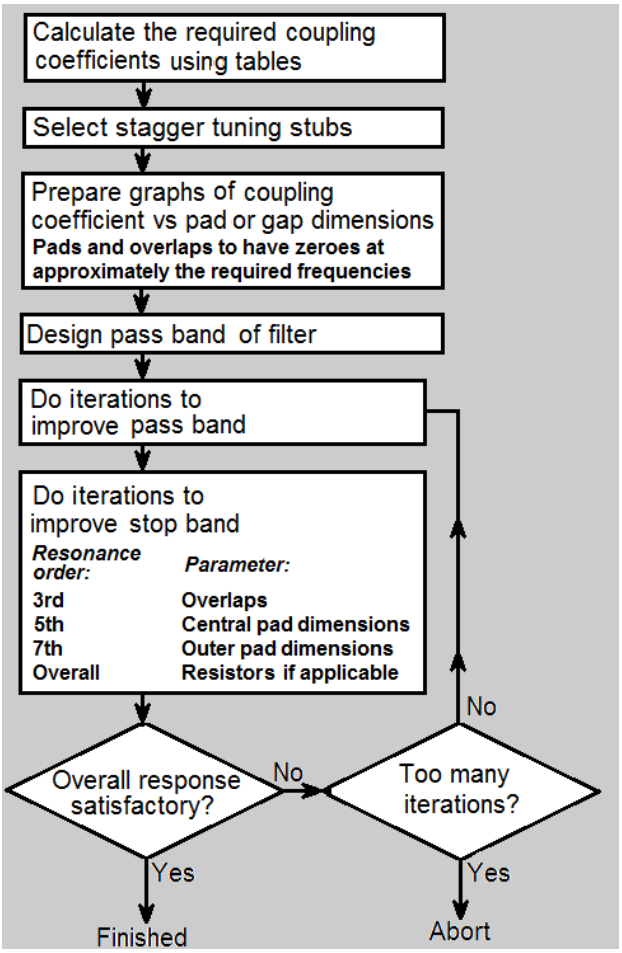

Fig. 7. Flow chart of the design procedure.

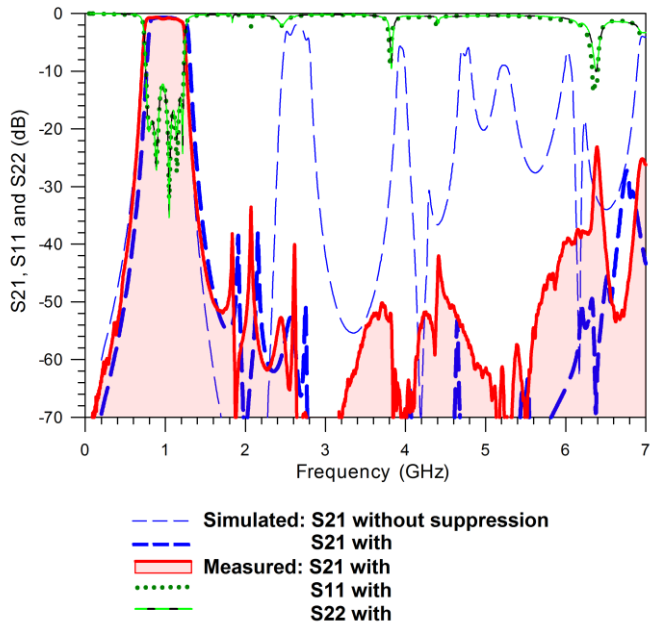

Fig. 8. Frequency response of the first filter, with no resistors.

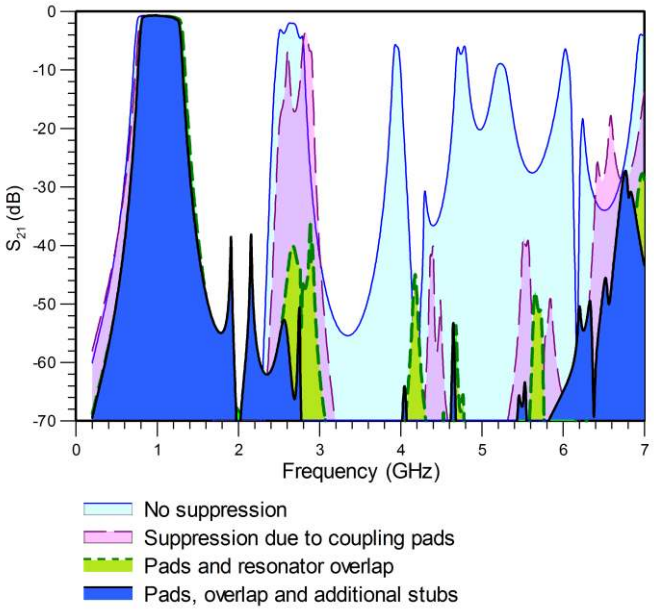

Fig. 9. Simulations of the available spurious suppression as the number of suppression techniques is increased

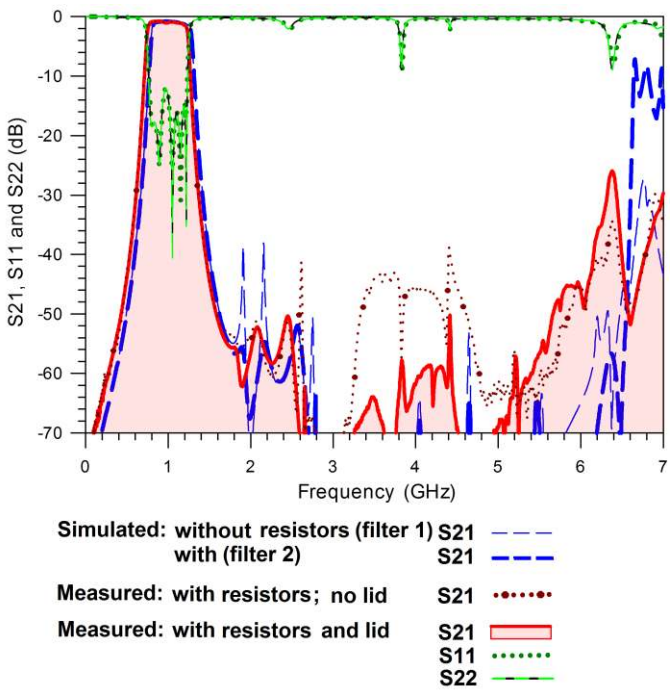

Fig. 10. Wide band frequency response of the second filter, with resistors.

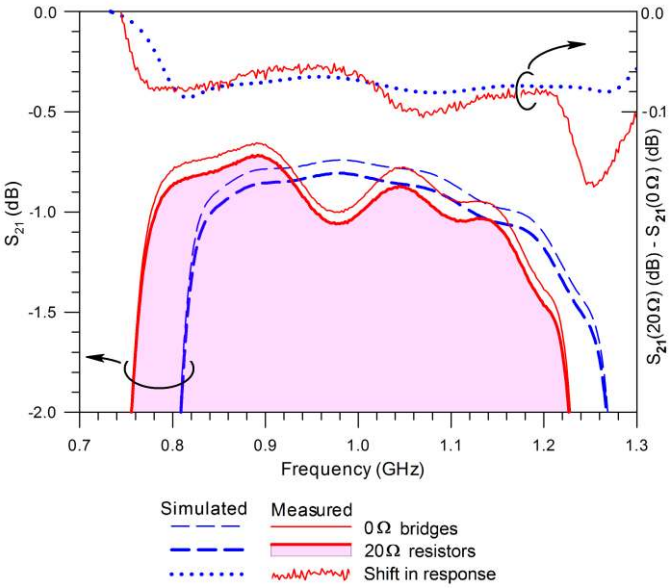

Fig. 11. Passband response of the second filter, showing the increase in insertion loss due to the two 20 Ω resistors, compared with 0 Ω bridges.

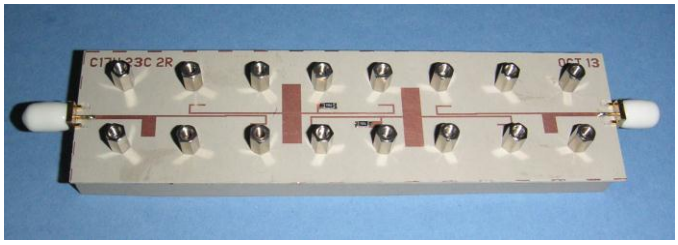

Fig. 12. The second filter, with cover removed. The 8 mm high posts are used in lieu of side walls. The first filter required neither posts nor cover. The cover is copper-clad PCB, with the same dimensions 150 mm x 40 mm as the substrate, and holes drilled to screw it to the posts.

The layout and final dimensions are shown in Fig. 1. The substrate is RT duroid with dielectric constant 10.2 and thickness 1.27 mm. The input and output are 50 Ω lines with width 1.25 mm. Resonator and stub line widths are 0.5 mm and 2 mm respectively. The gap between C and D is 0.625 mm. To avoid small simulation cell sizes, the separation between resonators A and B is 0.25 mm over half the distance, and 0.375 mm over the other half, instead of a uniform 0.3125 mm. The simulated response of the first filter is shown as the bold blue dashed line in Fig. 8. No spurious responses rise higher than -38 dB, up to 6.6 GHz. The peak at 6.7 GHz is due to the 9th order resonance of resonator A coupled to F; it is still present when the other resonators are deleted. It is significantly lower than the expected 9 GHz because some of the standing wave pattern is subsumed by the capacitive pad.

A major change which required a repeat of the design procedure was that the pad between resonators B and C was replaced by a center-fed pad as shown in Fig. 1. This is equivalent to two smaller pads in parallel, each with half the original area. The maximum useful frequency (the right hand side of figs. 5 and 6) was consequently extended upwards, to make use of a wider notch. Fig. 8 shows the final design including this change, and a corresponding change to the pad between resonators D and E.

The simulated response of a filter with no suppression is also shown. The resonators are straight with quarter-wave overlap. The outer pads have dimensions x=10 mm y=3 mm and the inner pads are 11 mm x 8.5 mm; $x>y$ is a bad choice as discussed in section IV. The improvement is evident.

The contribution of the various techniques is illustrated in Fig. 9, where the responses with and without suppression are compared with responses of filters with only some of the suppression methods. Except to make this comparison, only the filter with all the suppression needs to be designed. With no suppression, numerous peaks rise above -10 dB. In the second filter, the central pads reduce the 5th order resonances and the outer pads suppress the 7th order resonances, both to approximately -40 dB after the above design procedure has been followed. There has been no attempt at the 3rd order resonance. The next filter employs the same procedure, but with both the pads and the resonator overlap. The 3rd order resonance falls to -36 dB with little change to the others. Finally, the design with all three suppression techniques is shown. Comparing the resonances near 2.8 GHz (without stagger tuning) with those near 2 GHz (shifted there by the stagger tuning technique), the improvement is only 2 dB. Its main use here is to reduce sensitivity to fabrication errors. Two coincident spurious peaks require a nearly-coincident transmission zero, to be equivalent to only one peak. In contrast, if the peaks are well separated, the transmission zero can be placed half-way in between; its frequency error would have to take it all the way to one of the peaks before the response becomes as bad as the first case. As a result, the spurious response rises only 1 dB instead of 9.5 dB when the simulated overlap is changed by 0.125 mm, to estimate the effect of 0.125 mm fabrication error. Although the stubs also provide a place to solder on the resistors in filter 2, the stagger tuning is probably under-utilized.

Fig. 9 also shows that the 3rd, 5th and 7th order resonances occur at approximately 2.7, 4.4 and 5.6 GHz. Like the 9th order resonance the frequencies are lower than expected, for the same reason.

The second filter, if designed independently, would have followed the design procedure of Fig. 7, probably with the resistors included only in a third transit through the loop. However it was simpler to use the completed filter 1, and add two 20 Ω, 3.2 mm chip resistors to the stubs. Only the overlap between resonators C and D had to be re-adjusted. Fig. 10 concludes the progression of increasing the number of suppression techniques begun in Fig. 9. The two spurious peaks near 2 GHz are improved by 17 dB. Overall, attenuation is better than -52 dB up to 6.6 GHz. The average 0.07 dB increase in pass band loss due to the resistors is shown in Fig. 11.

VII. Filter Measurements

Measurements are given in Fig. 8 for the first filter without resistors. One practical detail is that the 4 mm earth pins of the SMA connectors resonated just below 6 GHz, because of the high dielectric constant of the substrate, and had to be shortened. Stop band spurious responses up to 6.3 GHz are reduced to -33.5 dB, short of the simulated -38 dB but still excellent performance. Comparing the peaks in the simulations and measured results, there is a 5% frequency error. Re-simulating with a scaled dielectric constant (whether or not it is the real cause of the discrepancy) the frequencies of the pass band, the spurious peaks and the upper stop band limits match very closely. The question of interpreting the data on dielectric constant is elaborated in [31].

The second filter is shown in Fig. 12. To benefit from the improved performance, a lid 8 mm above the substrate and metal posts in lieu of side walls were necessary to reduce the responses at 2.6 and in the range 3.2 to 4.4 GHz. Possible leakage out of the cavity, resulting from the sparsely placed posts, is not a difficulty provided that the coupling from the microstrip to the cavities is small. Wire bridges between the SMA connector earths and the lid were also required.

The measurements appear in Fig. 10. The resonance at 2.1 GHz has been improved to -52 dB, but it is no longer the worst response, so the overall level is -50 dB up to 5.6 GHz. The deterioration in pass band loss was confirmed to be 0.07 dB by comparing pass band magnitude before and after changing from 0 Ω bridges to the 20 Ω resistors (Fig. 11). Another measurement with 10 Ω resistors gives a -47.5 dB peak at 2.1 GHz with (in agreement with the simulation) 0.04 dB additional attenuation. The value is admittedly close to the measurement limit. Comparing 10 with 20 Ω resistors, the pass band loss is 40% less and the spurious suppression is 4.5 dB less, in approximate agreement with section V.

VIII. Conclusion

Spurious responses for wide band microstrip filters were effectively suppressed with a combination of techniques. The iterative design constitutes a basic level of optimization, but in a fully optimized filter, there may have been other trade-offs where (for example) the stubs are re-allocated to different resonators, or more stubs are used.

Table 1 compares some wide-band bandpass filters. (Medium width bandpass filters were compared in [1]). The

values of substrate permittivity ε_r and line width or gap width may be relevant to some designers considering feasibility of each filter type. Some values are very approximate, having been read off graphs or photographs; one value of minimum line width was estimated from the quoted characteristic impedance. Some of the small values of gap-to-substrate-thickness ratio are related to the tight coupling required for wide band width, and not to resonance suppression, as with the present work. Also, as previously described, the *g/h* ratio of 0.2 here could have been increased to 0.25 by using a uniform 0.3125 mm gap instead of a stepped gap of 0.25 mm and 0.375 mm. Each technique has its advantages, and the present work has the best attenuation level of the references found, a high stop band limit, and reasonable width-to-substrate-thickness ratio.

TABLE I
SOME WIDE PASS-BAND FILTERS WITH HARMONIC SUPPRESSION

	Mechanism	ε_r	*w/h* or *g/h* (a)	Band width (%)	Atten-uation (dB)	Stop-band limit (b)
[32]	Line width notches	4.4	0.13	30	48	(c) $2.4\,f_1$
[5]	Step impedance /capacitive load	4.7	0.11	20	40	$9.4\,f_1$
[1]	Stubs	10	0.4	22	37	$3.2\,f_1$
[33]	Position of cap input	10	0.08	28	20	$4.5\,f_1$
[24]	Loaded 90° line	3	0.2	97	31	$3\,f_1$
[25] (d)	Loaded 90° line	2.5	~1 (e)	95	15	(c) $5.2\,f_1$
[26] (d)	Loaded 90° line	11	~0.7	30	28	$2.5\,f_1$
[27]	SIR and IDC (f)	3.6	0.3	46	38	$4.3\,f_1$
This work	**Combination**	**10**	**0.2**	**42**	**50**	**$5.6\,f_1$**

(a) Smallest width-to-substrate-thickness or gap-to-thickness ratio
(b) The center of the pass band is f_1.
(c) Highest frequency shown on graph; stop band limit may be higher
(d) DC band not suppressed
(e) Estimated from a small photograph
(f) SIR = Stepped Impedance Resonator
IDT = Inter-Digital Capacitor

Additional design equations were required for the coupling capacitor pads acting as wide quarter wave stubs at the spurious frequencies. Modifications were also introduced for additional stubs that stagger tuned the higher order resonances and for selective attenuation of resonances using resistors. Resonator overlap was adopted with very little change.

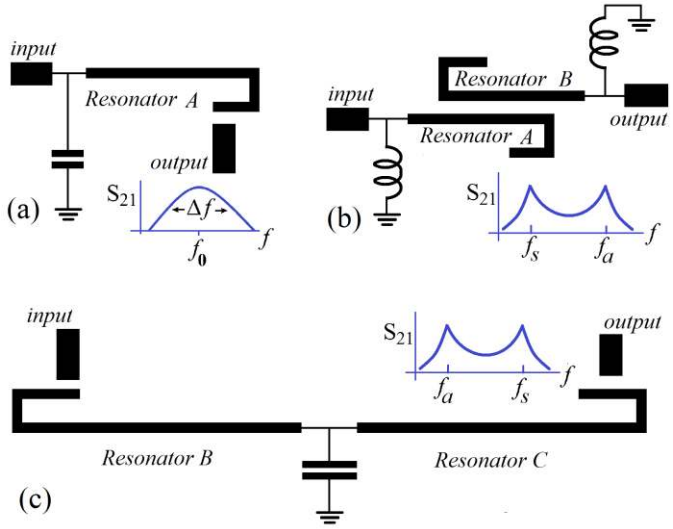

Fig 13. Schematic layouts for simulations to find (a) external coupling (b) coupling between two parallel coupled resonators and (c) two capacitor-coupled resonators.

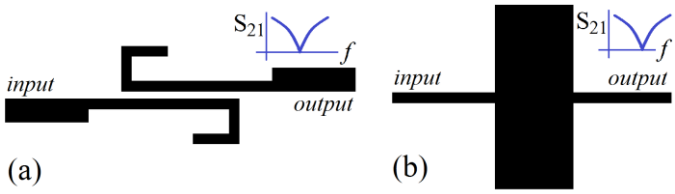

Fig 14. Schematic layouts for simulations to find zero coupling at the higher order resonances for (a) parallel- and (b) pad-coupled resonators.

APPENDIX: SIMULATIONS FOR COUPLING COEFFICIENTS AND TRANSMISSION NULLS

Schematic layouts for simulations to find coupling coefficients are given in Fig. 13. In Fig. 13(a), simulations give S_{21} which has a broad peak, and the external coupling factor k_e (more often denoted by the reciprocal of the external quality factor, $1/Q_e$) is

$$k_e = \frac{1}{Q_e} = \frac{\Delta f}{f_0} \qquad (10)$$

where Δf is the 3 dB bandwidth and f_0 the centre of the resonance. A design graph is prepared giving k_e for various values of capacitor pad area. The frequency zeroes for suppressing higher order resonances is not precisely known at this stage, and a very crude estimate is taken to decide the capacitor pad shape.

Fig. 13(b) gives the coupling coefficient of two parallel resonators. The inductors represent the inductance of vias to ground. In this simulation, external coupling should be small, so either small inductances or large capacitances are required; inductors are simpler. First considering the third harmonic, simulation gives two peaks in S_{21} which are the symmetric and antisymmetric third-harmonic modes. Varying the overlap for a fixed gap, coupling is minimized by having these two peaks as close as possible. This gives a first approximation for the overlap required for third harmonic suppression. Simulations do not have to be repeated for other gaps as the required overlap is reasonably constant. Turning to the fundamental frequency, simulations are made for varying gaps and the coupling coefficient is given by the symmetric f_s and anti-symmetric f_a mode resonances, based on (11.04-7) in [30],

$$k \approx \frac{|f_s - f_a|}{0.5(f_s + f_a)} \qquad (11)$$

and a graph of k against gap is prepared.

Finally Fig. 13(c) is used for the coupling coefficient between two resonators joined by a capacitive pad. A good approximation for k is found from (11) even with the stub not yet connected.

Before making iterative adjustments to the overlap in the whole filter, it is useful to observe simulated responses S_{21} of the much simpler structures shown in Fig. 14, to find the suitable overlap and pad dimensions to place nulls at a particular frequency (similar to Fig. 5). Convergence is rapid because it is known that the frequency of the nulls is approximately inversely proportional to the overlap, or to vary as (4) for the pad.

REFERENCES

[1] F. Huang, "Suppression of Harmonics in Microstrip Filters with Stagger Tuning and Voltage Redistributions", *IEEE Trans. Microw. Theory Techn.*, vol. 62, no. 3, pp. 464-471, Mar 2014.

[2] S.-C. Lin, P.-H. Deng, Y.-S Lin, C.-H. Wang and C. H. Chen, "Wide-stopband microstrip bandpass filters using dissimilar quarter-wavelength step-impedance resonators", *IEEE Trans. Microw. Theory Techn.*, vol. 54, no. 3, pp. 1011-1018, Mar 2006.

[3] C.-F. Chen, T.-Y. Huang, and R.-B. Wu, "Design of microstrip bandpass filters with multiorder spurious-mode suppression", *IEEE Trans. Microw. Theory Techn.*, vol. 53, no. 12, pp. 3788-3793. Dec 2005.

[4] M. Makimoto and S. Yamashita, "Half-wavelength-type SIR" in *Microwave resonators and filters for wireless communications*, Berlin: Springer Verlag, 2001. ISBN 9783642087004.

[5] W. M. Fathelbab and M. B. Steer, "Parallel-coupled line filters with enhanced stopband performances", *IEEE Trans. Microw. Theory Techn.*, vol.53, no. 12, pp. 3774-3781, Dec. 2005.

[6] M. Makimoto and S. Yamashita, "Bandpass filters using parallel coupled stripline stepped impedance resonators", *IEEE Trans. Microw. Theory Techn.*, vol. MTT-28, no. 12, pp. 1413-1417, Dec. 1980.

[7] W.-H. Tu, H. Li, K. A. Michalski and K. Chang, "Microstrip Open-Loop Ring Bandpass Filter Using Open Stubs for Harmonic Suppression", in *IEEE MTT-S Int. Microw. Symp. Dig.,* San Francisco, 2006, pp 357-360.

[8] K.-W. Hsu, M.-J. Tsou, Y.-H. Tseng, and W.-H. Tu, "Wide-Stopband Bandpass Filter with Symmetrical Loaded-Stub Resonators", in *Proc Asia-Pacific Microw. Conference*, 2011, pp1043-1046.

[9] A. Griol, J. Marti and L. Sempere, "Microstrip multistage coupled ring bandpass filters using spur-line filters for harmonic suppression", *Electronics Lett.,* vol. 37, no. 9, pp. 572-573, Apr. 2001.

[10] S. Hong and K. Chang, "A parallel-coupled microstrip bandpass filter with suppression of both the 2nd and the 3rd harmonic responses", in *IEEE MTT-S Int. Microw. Symp. Dig*., San Francisco, 2006, pp 365-368.

[11] J.-T. Kuo, S.-P. Chen, and M Jiang, "Parallel-coupled microstrip filters with over-coupled end stages for suppression of spurious responses", *IEEE Microw Wireless Compon Lett.,* vol. 13, no. 10, pp. 440-442, Oct. 2003.

[12] P. Cheong, S.-W. Fok, and K.-W. Tam, "Miniaturized Parallel Couple-Line Bandpass Filter With Spurious-Response Suppression", *IEEE Trans. Microw. Theory Techn.*, vol.53, no. 5, pp. 1810-1816, May 2005.

[13] A. Riddle, "High performance parallel coupled microstrip filters", in *1988 IEEE MTT-S Int. Microw. Symp. Dig.*, 1988, pp. 427 – 430.

[14] A. Afkhami, G. Askari, Atefeh Kordzadeh and Hamid Mirmohammad Sadeghi, "Second and third harmonic suppression in parallel coupled line filter using sliding coupling", in *Proc. 40th European Microw. Conference*, Paris, France, Sep 2010, pp.759-762.

[15] M.A. Sanchez-Soriano, G. Torregrosa-Penalva and E. Bronchalo, "Multispurious Suppression in Parallel-Coupled Line Filters by Means of Coupling Control", *IET Microw., Antennas Propag.,* vol. 6, no. 11, pp. 1269-1276, 2012.

[16] X. D. Huang and C.H. Cheng, "A novel microstrip dual-mode bandpass filter with harmonic suppression", *IEEE Microw Wireless Compon Lett.,* vol. 16, no.7, pp. 404-406, Jul. 2006.

[17] J.-R. Lee, J.-H Cho, and S.-Won Yun, "New compact bandpass filter using microstrip λ/4 resonators with open stub inverter", *IEEE Microw. Guid. Wave Lett.,* vol. 10, no.12, pp. 526-527, Dec. 2000.

[18] L. Zhu, and W. Menzel, "Compact microstrip bandpass filter with two transmission zeros using a stub-tapped half-wavelength line resonator", *IEEE Microw Wireless Compon Lett,* vol. 13, no.1, pp. 16-18, Jan. 2003.

[19] W.-H. Tu, "Compact double-mode cross-coupled microstrip bandpass filter with tunable transmission zeros", *IET Microw., Antennas and Propag*., vol. 2, no. 4, pp. 373-77, Apr. 2008.

[20] L. Zhu, S. Sun, and W Menzel, "Ultra-wideband (UWB) bandpass filters using multiple-mode resonator", *IEEE Microw. Wireless Compon. Lett.,* vol. 15, no. 11, pp. 796-798, Nov. 2005.

[21] F. Huang, "Suppression of Superconducting Filter Spurious Response Using Lossy Parasitic Resonators", *IET Microw., Antennas and Propag.,* vol. 4, no. 12, pp. 2042-2049, Dec. 2010.

[22] F. Huang, "Suppression of Microstrip Filter Spurious Responses Using Frequency-Selective Resistive Elements", *IET Microw., Antennas and Propag.,* vol. 5, no. 15, pp. 1836-1843, 2011

[23] F. Huang, "Suppression of Spurious Responses in Microstrip Filters Using a Reduced Number of Resistors" *IET Microw. Antennas and Propag.,* vol. 6, no. 10, pp. 1128-1135, Jul. 2012.

[24] H. N. Shaman and J.-S. Hong, "Compact wideband bandpass filter with high performance and harmonic suppression", in *Proc. 37th European Microw. Conference*, Munich, Germany, Oct 2007, pp. 528-531.

[25] Y.-G. Choi and B.-Ki. Kim, "Design of a 5.8 GHz broadband BPFs with second harmonics suppression using open-stubs", ", in *Proc. Asia-Pacific Microw. Conference*, 2017, Bangkok, Thailand, pp. 1-4.

[26] W.-H. Tu and K. Chang, "Compact second harmonic-supppresed bandstop and bandpass filters using open stubs", *IEEE Trans. Microw. Theory Techn.*, vol. 54, no. 6, pp. 2497-2502, Jun. 2006.

[27] C.-H. Liang and C.-Y. Chang, "Compact wideband bandpass filters using stepped-impedance resonators and interdigital coupling structures", *IEEE Microw. wireless compon. let.,* vol. 19, no. 9, pp. 551-553, Sep. 2009.

[28] P. Mondal and M. K. Mandal, "Design of Dual-band bandpass filters using stub-loaded open-loop resonators", *IEEE Trans. Microw. Theory Techn.*, vol. 56, no. 1, pp. 150-155, Jan. 2008.

[29] S.B. Cohn, "Dissipation loss in multiple-coupled-resonator filters", *Proc. IRE*, vol. 47, no. 8, pp.1342-1348, Aug. 1959.

[30] G. Matthaei, L. Young, and E. M. T. Jones, "Microwave Filters, Impedance-Matching Networks, and Coupling Structures" Norwood, MA: Artech House, 1980, pp. 100, 432 and 666.

[31] (No stated author) "General information of dielectric constant for RT/duroid® 6010.2LM & RO3010™ High frequency circuit materials" Accessed 22 Sep 2014. Available: http://www.rogerscorp.com/documents/2379/acs/General-Information-of-Dielectric-Constant-for-RT-duroid-6010.2LM-RO3010-High-Frequency-Circuit-Materials.pdf

[32] J. Marimuthu and M. Esa, "Wideband and harmonic suppression method of parallel coupled microstrip bandpass filter using centered single groove", in *Proc. 2007 IEEE Int. Conference on Telecommun. and Malaysia Int. Conference on Commun.,* Penang, Malaysia, pp622-626, May 2007.

[33] W. Nie, S. Luo, Y. Guo and Y. Fan, "Compact bandpass filter with improved upper stopband", *Electronics Lett.,* vol. 50, no. 15, pp. 1065-1067, Jul 2014.

Frederick Huang received the B.A. and D. Phil degrees in Engineering Science from the University of Oxford in 1980 and 1984. Since 1989 he has been a lecturer with the University of Birmingham.

Previous research interests are surface acoustic wave (SAW) dot array pulse compressors, analogue voice scramblers, Langmuir-Blodgett films, SAW and superconducting linear phase and chirp filter synthesis using inverse scattering, slow-wave structures, superconducting quasi-lumped element filters, switched filters and delay lines, together with microstrip and waveguide discontinuities. The main current interests are spiral band-pass filters and filter harmonic suppression.

Dr. Huang is a member of the IET (UK).